

# VISUAL INSPECTION OF CURVED PARTICLE ACCELERATOR BEAM PIPES WITH A MODULAR ROBOT

N. Schweizer\*, RMR, Technische Universität Darmstadt, Germany

I. Pongrac, GSI Helmholtzzentrum für Schwerionenforschung GmbH, Darmstadt, Germany

## Abstract

Inspecting ultra-high vacuum pipe systems of particle accelerators without disassembling the beam pipes is a complex challenge. In particular, curved sections of particle accelerators require a unique approach for the examination of the interior. For the planned heavy ion synchrotron SIS100 at FAIR, an inspection robot is currently under development, featuring an optical imaging system with which the robot can be navigated through the beam pipe. We present the current prototype, which is based on a modular snake-like robot with active wheels and joints. Due to the stipulated low movement velocity, it can be shown that a kinematic model is sufficient to control the robot whereas dynamical effects can be neglected. This concept is proven in experiments with the prototype. At the current development status, the robot is controlled manually by setting the velocity of the first module and its desired turning angle. In simulations we include a CAD model of a dipole chamber of the SIS100 and let an operator successfully navigate the robot through the beam pipe while only observing the camera image.

## INTRODUCTION

Considering the ultra-high vacuum system of ring accelerators, the vacuum pipes can be divided into straight and curved accelerator pipes. Periodic visual inspection of both types of pipes allows to collect information about material conditions and foreign objects inside the system. These data can help to ensure the integrity of the vacuum system and are essential for unimpaired beam experiments.

To minimize the effort and the expenditure of time for the examination of the beam vacuum system of particle accelerators, an inspection device is being developed that shall be introduced into the pipe system. At the current development status a modular robot platform is designed for the use in straight accelerator pipes and to negotiate simple obstacles like gaps and single steps between two pipe sections [1]. A prototype was built and adapted to the pipe geometry of the heavy ion synchrotron SIS100 of the international accelerator facility FAIR. The robot prototype consists of four modules, each equipped with two independently driven wheels. Pitch rotational joints between the modules and specified wheel positions enable the robot to overcome the obstacles successfully.

Next, the development is focused on the inspection of curved beam pipes, i.e. of dipole chambers of the SIS100. In order to navigate the robot through this type of pipes, turning capabilities are needed. In the following a suitable robot design is presented and its associated kinematic model,

which is used to control the robot, is explained. Finally, the control and the behavior of the robot is evaluated.

## ROBOT DESCRIPTION

Concerning homogeneous dipole chambers, the turning problem can be considered separately from the previous prototype of the robot with climbing capabilities. However, the final inspection device should include both turning and climbing skills. Hence, the already developed robot structure must be kept as far as possible. Moreover, when a turning mechanism is added, the robot dimensions must still satisfy the feasible height of 50 mm and the maximum width of 60 mm. Otherwise the robot would not fit into the dipole chamber beam pipes of the SIS100.

Instead of introducing direct steering on the wheels, the pitch joints are replaced with active yaw joints, which fit without further changes into the existing robot structure. Later, the pitch joints can be easily added again.

The current robot prototype with yaw joints is shown in Fig. 1 and is constructed with four 3D printed modules like the previous prototype. Thus, in total three joints are integrated. The two inner modules carry a battery and most of the electronic components like a microcontroller, voltage regulators and a communication module to receive control commands wirelessly. The combination of the active joints and the active wheels enables the robot to turn. This concept is known for example from the snake-like robots PiKo [2] and MoMo [3].

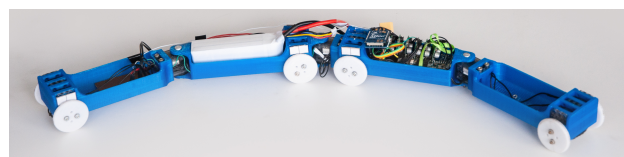


Figure 1: Prototype of the robot with turning capabilities.

## Motion Control

Without steerable wheel axles, the robot turns into a desired direction only by coordinated control of the joints and the wheel velocities. From a given velocity of the first robot module  $v_{w_1}$  and a turning angle  $\delta_1$ , joint angles and wheel velocities for the other modules can be algebraically calculated. A kinematic model of a modular robot with active wheels and joints is fully described in [4] using the example of the robot PiKo. For our robot we have to adjust the model slightly, because PiKo is equipped with identical modules, i.e., the distances between the wheel axle of a module and the connected joints are the same for each module. Consequently, all modules are of the same length. In our robot,

\* nicolai.schweizer@rmm.tu-darmstadt.de

Any distribution of this work must maintain attribution to the author(s), title of the work, publisher, and DOI (© 2019). Content from this work may be used under the terms of the CC BY 3.0 licence (© 2019).

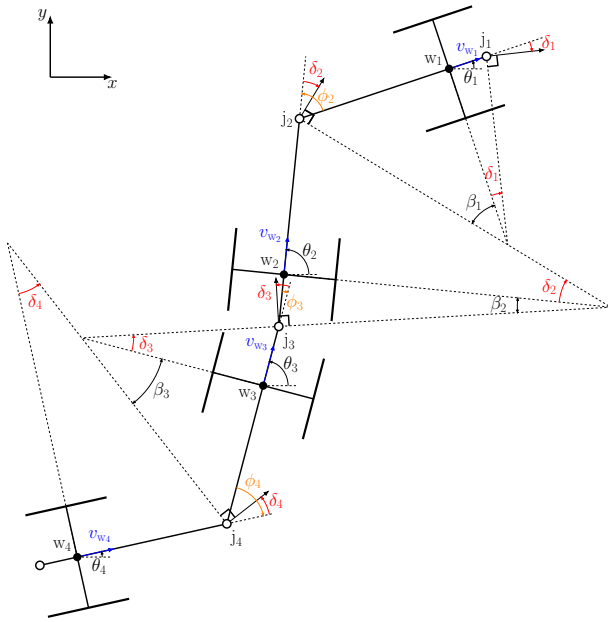


Figure 2: Geometric relations and model parameters of the robot with four modules, based on [4].

the lengths are different and the wheel positions vary. Therefore, we use a slightly more general description of the robot kinematics that takes the different module geometries into account.

The angular velocity of a module  $i = 1, \dots, n$  is

$$\dot{\theta}_i = \frac{v_{w_i}}{l_{w_i j_i}} \tan \delta_i, \quad (1)$$

with the desired moving direction  $\delta_i$  of module  $i$  and the module velocity  $v_{w_i}$ . The length  $l_{w_i j_i}$  describes the distance from wheel axle  $w_i$  to joint  $j_i$  or to the robot head in the case of  $l_{w_1 j_1}$ .

From Fig. 2 the relations

$$\tan \beta_i = -\frac{l_{w_i j_{i+1}}}{l_{w_i j_i}} \tan \delta_i \quad (2)$$

and

$$\delta_{i+1} = \beta_i - \phi_{i+1} \quad (3)$$

can be derived, where  $\phi_i$  denotes the joint angle. The related angular velocities of the joints are

$$\dot{\phi}_i = -v_{w_{i-1}} \left[ \frac{\sin \phi_i}{l_{w_i j_i}} + \frac{\tan \delta_{i-1}}{l_{w_{i-1} j_{i-1}}} \left( \frac{l_{w_{i-1} j_i}}{l_{w_i j_i}} \cos \phi_i + 1 \right) \right]. \quad (4)$$

Finally, module velocities are given by

$$v_{w_{i+1}} = v_{w_i} \frac{\cos \delta_{i+1}}{\cos \beta_i}. \quad (5)$$

Starting from the first module with  $v_{w_1}$  and  $\delta_1$ , calculation of the module parameters is done iteratively, because module  $i+1$  depends on the parameters of module  $i$ . Therefore, an arbitrary number of modules can be added to extend the robot, if more space is needed, for example for additional batteries, sensors or tools.

## EVALUATION

### Kinematic Model

Assuming a slow locomotion with a maximum velocity of  $v_{w_1} = 0.05$  m/s, the robot is controlled only by the kinematic model, while forces, friction and other dynamic effects can be neglected. This approach obviates the need for a sophisticated parameter identification, but this has to be proven.

To assess the accuracy of the kinematic model, multiple experiments were conducted with the robot prototype on a flat surface. While the robot was controlled with a constant turning angle in the range from  $\delta_1 = -2^\circ$  to  $\delta_1 = 2^\circ$  and constant velocities from  $v_{w_1} = 0.02$  m/s to  $v_{w_1} = 0.05$  m/s, a camera tracking system recorded the actual positions of the robot head. Then, these measurements were compared with the simulated output of the kinematic model.

As an example, the comparisons for a turning angle of  $\delta_1 = 1.5^\circ$  and  $\delta_1 = -1.5^\circ$  are depicted in Fig. 3. In these two experiments the robot was driven with a velocity of  $v_{w_1} = 0.05$  m/s. A positive turning angle means steering to the left and for a constant angle driving a circle counterclockwise. For a negative turning angle the robot steers to the right and drives a circle clockwise, respectively. The red circle in the figure has a radius of 0.573 m and shows the ideal path, calculated by the kinematic model. The trajectory in blue was recorded for  $\delta_1 = 1.5^\circ$  and coincides almost with the reference trajectory. Comparing the radii of both circles the error is only about 0.19%. For the clockwise movement of the robot, which is displayed in green, the driven circle is slightly larger and results in an error of 1.02%.

The maximum measured error from all experiments was about 2%. Accordingly, the robot prototype navigates very precisely, which is particularly due to the well tuned motor controllers. Nevertheless, it should be mentioned that errors

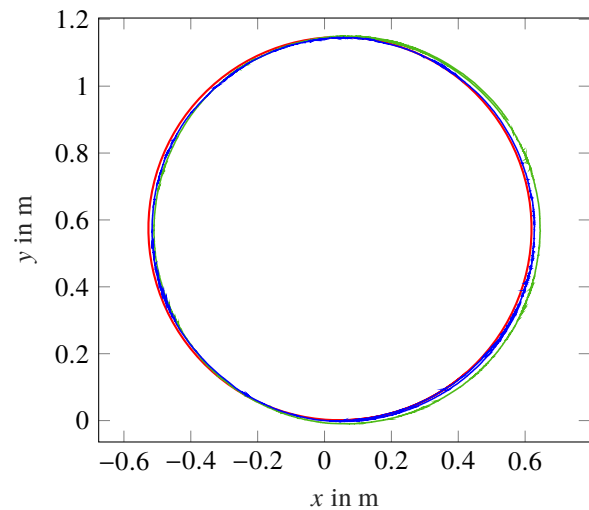


Figure 3: Driven circles of the robot for  $\delta_1 = 1.5^\circ$  in blue and  $\delta_1 = -1.5^\circ$  in green at a velocity of 0.05 m/s and reference trajectory in red.

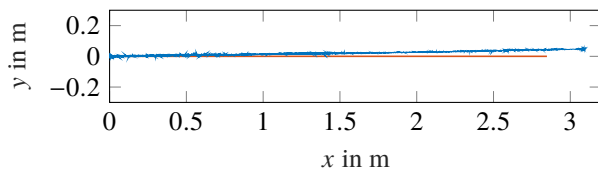


Figure 4: Simulated position in red and tracked position of the prototype in blue for driving straight.

of clockwise driven circles were always a bit larger than the errors of the corresponding counterclockwise driven circles. Furthermore, if a turning angle of  $\delta_1 = 0^\circ$  is set, the robot will not move exactly straight as Fig. 4 illustrates. Instead, it heads slightly to the left, which is also the reason for the difference in the error of the two moving directions. However, the deviations are very small and acceptable for the robot control in a beam pipe. Thus, the approach of using only a kinematic model to calculate the control commands has proven to be convenient.

### In-pipe Navigation

Despite the good results described above, the experiments were all performed only on flat surfaces. Next, the robot behavior within a pipe environment is considered. Additionally, the robot is controlled manually, i.e. an operator sets the robot velocity and the turning angle, which are both used as inputs for the kinematic model. For the experiments, 3D robotic simulation and a CAD model of a SIS100 dipole chamber are used. To be even more realistic, the operator observes only the image of a camera that is attached to the robot head. Moreover, a lamp is added to light the beam pipe.

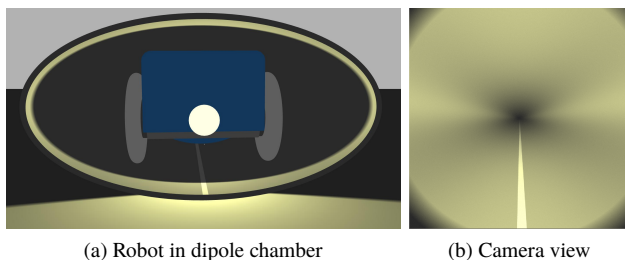


Figure 5: Robotic simulation in Gazebo with a CAD model of a SIS100 dipole chamber.

In Fig. 5a the robot is leaving the dipole chamber. Here, the lamp illuminates the edge of the chamber. On the second image in Fig. 5b the camera view is displayed while moving through the pipe. This live image is used by the operator to navigate the robot. A clear line is drawn on the bottom of the pipe that serves as a reference for the robot orientation. Due to the large bending radius of the dipole chamber (52.632 m), without such a marker it is almost impossible to recognize when the robot needs to be steered, because the image would look the same for different orientations. Even with the elliptical shape of the chamber, deviations from the pipe center cannot be detected.

Multiple simulations have proven a successful control of the robot through the curved dipole chamber. The comparison in Fig. 6 between the ideal path in the middle of the pipe and the real position of the robot head shows just small deviations. In this example, the largest magnitude of deviation is only about 1.5 mm. Furthermore, minor control corrections are sufficient to keep the robot close to the ideal path.

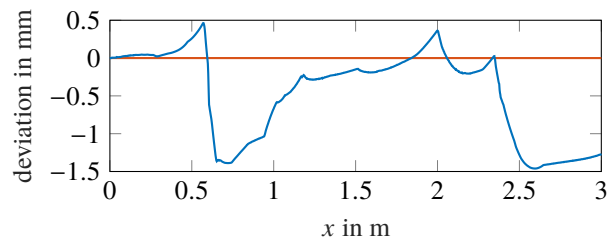


Figure 6: Deviation of the robot head from the ideal path.

## CONCLUSION AND OUTLOOK

Inspecting curved pipe sections can be generally done with the presented robot concept. Moreover, movements of the prototype are sufficiently described by the kinematic model and test operators succeeded in controlling the robot manually through a SIS100 dipole chamber. However, in simulations the manual control depends on a marker that designates an orientation in the pipe. For real inspections of the SIS100 it must be checked if the beam pipes show any material structure that can be used as guidance. Otherwise manual control with the camera image will not be possible.

Besides, test operators had to be very concentrated all the time to discern and compensate deviations from the ideal path. Due to that effort operating errors can easily occur. Therefore, the next development step will be focused on autonomous lane keeping in straight and curved accelerator pipes. By including an inertial measurement unit, the roll angle of the robot can be measured and used for navigation. Furthermore, the roll angle can also be used for manual control to navigate the robot without the need of a marker in the camera image.

## REFERENCES

- [1] N. Schweizer and I. Pongrac, "Autonomous topography detection and traversal for an inspection robot within the beamline of particle accelerators", in *Proc. IPAC'18*, Vancouver, Canada, May 2018, paper THPAL128, pp. 3943–3945.
- [2] S.A. Fjerdings, P. Liljebäck and A.A. Transth, "A snake-like robot for internal inspection of complex pipe structures (PIKo)", in *IEEE/RSJ Int. Conf. Intelligent Robots, Systems*, St. Louis, MO, 2009, pp. 5665–5671.
- [3] T. Khunnithiwarawat and T. Maneewarn, "A study of Active-Wheel snake robot locomotion gaits", in *IEEE Int. Conf. Robotics, Biomimetics*, Karon Beach, Phuket, 2011, pp. 2805–2809.
- [4] B. Murugendran, A. A. Transth and S. A. Fjerdings, "Modeling and path-following for a snake robot with active wheels", in *IEEE/RSJ Int. Conf. Intelligent Robots, Systems*, St. Louis, MO, 2009, pp. 3643–3650.